

Heat transfer optimization of MHD convection in enclosure heated by symmetrical heaters separated by a triangular slab via SRT-BGK model

Taoufik Naffouti^{1, 2, 3, 4†}, Lamia Thamri^{1, 2} and Ridha Djebali^{5, 6}

¹ University of Tunis El-Manar, Faculté des Sciences de Tunis, Département de Physique, Tunis, Tunisia

² Laboratoire d'Energétique et des Transferts Thermique et Massique, El Manar 2092, Tunis, Tunisia.

³ Institut Préparatoire aux Etudes d'Ingénieurs El-Manar, El-Manar 2092, Tunis, Tunisia.

⁴ College of Sciences and Humanities of Dawadmi, Shaqra University, Shaqra, Kingdom of Saudi Arabia

⁵ University of Jendouba, ISLAIB, Boulevard of the Environment, BP 340, Béja-9000, Tunisia .

⁶ LR: Subatomic Physics, Nanoscience and Energetics, University of Carthage, Tunis-2070 , Tunisia

†Corresponding author: Taoufik Naffouti

Abstract

SRT-BGK model of LBM is applied to predict thermal and dynamic characteristics of free convection under a Lorentz force inside an enclosure heated isothermally from below by two symmetrical heaters. Vertical walls of the enclosure and the triangular slab localized between heaters at the middle are considered cold while other walls are maintained adiabatic. Computed results are performed for air in a wide range of Rayleigh number ($Ra = 10^3$ to 10^6), Hartmann number ($Ha = 0$ to 80) for three inclination angle of the magnetic field ($\alpha = 0^\circ, 45^\circ$ and 90°). Current computations are validated with available previous researches related to the problem. It is found that the physics of MHD convection and heat transfer is strongly affected by the inclination angle α and Ha at $Ra = 10^5$. The growth of Lorentz force intensity conduct to neglect the convection and to destroy the interaction between two thermal plumes is obtained. For $Ra = 10^5$, the optimization of heat transfer shows that the Nusselt number vs magneto-convective parameter ε is highest for the case of vertical magnetic field corresponding to $\alpha = 90^\circ$ while it is weaker for case of horizontal magnetic field.

Keywords: MHD convection, thermal plumes, triangular slab, heat transfer, optimization, SRT-BGK of LBM.

Date of Submission: 24-09-2020

Date of Acceptance: 06-10-2020

I. INTRODUCTION

Natural convection heat transfer of fluids evolving inside confined locations in the absence of magnetic field has been the object of diverse investigations owing to its large applications for many thermal systems such as heat exchanger, heating/cooling of building, cooling of electronic equipment and others [1-16]. The literature review show that flow behavior and their heat transfers are influenced by wide parameters monitoring this one; Rayleigh and Prandtl numbers, inclination angle, enclosure aspect ratio, heater size and so on...

For previous two decades, some researchers are carried out numerical and experimental investigations of laminar buoyant convection of electrically conducting fluids under a magnetic field. Findings related to the problem can be use to improve performances of various practical technological and engineering applications [17-26]. The existence of magnetic force witch interacts with the buoyancy force conducts to neglect the convection and to weaken the dynamic of the fluid. Hence, the addition of Lorentz force can help to control different systems such as cooling of electrical systems, solar cells, growing crystals in liquids, etc. Convective flow inside a 2-D enclosure under a magnetic field with different orientations is carried out by A.Y. Gelfgat and P.Z. Bar-Yoseph [27]. They found that the flow is more stabilized in a presence of transversal magnetic field. MHD convection in a 2-d cavity subject to a vertical magnetic field is analyzed by J.P. Garandet et al.[28] using an analytical solution. After, T. Tagawa et al.[29] applied a Lorentz force to free convection of air inside a cubic box. By studying the influence of magnetizing force on air in a gravitational field inside a two dimensional cylindrical container, M. Akamatsu et al.[30] prove that the conduction is significant for higher Ha . Then, I.E. Sarris et al.[31] analyzed the effect of longitudinal magnetic field on unsteady natural convection in a differentially heated enclosure. After, I.E. Sarris et al.[32] focused their attention to the study of MHD convection in the same enclosure but in the presence of a transversal magnetic field. Afterward, T. Bednarz et al.[33] examined free convection of paramagnetic fluid under a longitudinal magnetic field in a 3-D medium. Via the control volume method, P. Kandaswamy et al. [34] numerically elucidated the magneto-convection in a square cavity laterally heated by one side. For higher Ha , the addition of vertical Lorentz force

leads to neglect the heat transfer convection for various Gr. Using VF approach, M. Pirmohammadi et al. [35] investigated buoyancy-driven convection under a longitudinal magnetic field in a square enclosure heated from left vertical wall. For $Pr = 0.733$, numerical predictions show that the flow behavior is affected by Ha. Then, T. P. Bednarz [36] applied a transverse magnetic field on free convection of a paramagnetic fluid inside a differentially heated cubic cavity. For the same period M. Pirmohammadi and M. Ghassemi [37] numerically simulated the effect of Ha on natural convection in an inclined cavity filled with liquid gallium.

D.C. Lo [38] examined buoyancy-driven MHD flow in a differentially heated cavity under a vertical Lorentz force. At a fixed Gr, the growth of Ha causes an attenuation of the Nusselt number for the lower Prandtl number. Then, M. Sathiyamoorthy and A.J. Chamkha [39] adopted the FE method to delineate natural convection of conducting liquid gallium under an inclined magnetic field inside a square enclosure heated from below and on sides. Using TLB model, R. Djebali et al.[40] analysis free convective in saturated porous tilted square cavity for various directions of Lorentz force. After, Z.Jing et al.[41] applied a Lorentz force on liquid metal in 3-D cavity. Various directions of a constant Lorentz force are employed. To analysis the behavior of liquid mercury in a 2-D enclosure for various directions of Lorentz force, P.X.Yu et al.[42] resolved equations governing the flow via DF method. For a fixed $Pr = 0.025$, computations prove that flow characteristics depend to Ha and the direction of Lorentz force. After that, K. Song et al. [43] performed a numerical study on MHD free convection under a uniform magnetic field inside a square cavity.

Using DF and LB approaches, G.H.R.Kefayati [44] delineated free convection under a horizontal magnetic field in an enclosure discretely heated. The problem of convection melting of solid gallium in a 2-D enclosure heated from the bottom with transversal/longitudinal magnetic field is simulated by Y.Feng et al. [45]. Using LBM, they noted that flow characteristics are influenced by inclination angle of magnetic field and Ha. J.Zhang et al.[46] numerically elucidated free convection in an enclosure versus magnetic field intensity. Results show that fluid characteristics are influenced by thermal radiation and Lorentz force. Using EF approach, S.Alam et al.[47] focused their researches on 2-D free convection under Lorentz force in a rectangular enclosure heated from bottom. For $Pr = 0.71$, computations show that flow behavior greatly affected by Ra and the intensity of Lorentz force. Through EF method, A.J.Chamkha and F.Selimefendigil [48] investigated natural convection inside a corrugated porous and differentially heated enclosure with Cu-water nanofluid under vertical magnetic field. A reduction of convective heat transfer is deduced as increasing Ha. Then, C.Haritha et al.[49] analyzed free convection of nanofluid in saturated porous square enclosure heated by sides under a horizontal Lorentz force. T.R.Mahapatra and P.Rujda [50] examined the effect of vertical magnetic field on convective heat transfer in a differentially heated cavity filled with Cu-water nanofluid. It is found that the dynamic of the flow is strongly influenced by the variation of Ha. Using the approach of LB, H.Sajjadi et al.[51] delineated the air under Lorentz force in confined medium. For $Pr = 0.73$, numerical results prove that the effect of the Lorentz force intensity increases as increasing the Ra.

The present numerical investigation deals with the free convection heat transfer in the absence/presence of a uniform magnetic field in a rectangular enclosure heated from below via tow symmetrical discrete heaters localized on sides of a cold triangular slab. The enclosure is filled with an electrically conducting fluid and the Prandtl number is fixed at 0.71. Three orientations of the magnetic field are applied; horizontal, inclined and vertical to gravity. The single relaxation time Bhatnagar-Gross-Krook (SRT-BGK) model of Lattice Boltzmann method (LBM) is employed. The main object of the study is to analysis effects of intensity and angle inclination of a magnetic field on thermal and dynamic characteristics of the flow in order to optimize the heat transfer.

II. MATHEMATICAL FORMULATION

2.1 Problem description

The studied configuration related to the present problem with boundary conditions is illustrated in Fig. 1. It is a 2-D rectangular enclosure of aspect ratio $L/H = 2$ filled with an incompressible electrically conducting fluid under magnetic field. The working fluid of Prandtl number fixed at 0.71 is heated via tow heaters S_1 and S_2 maintained at a constant temperature T_h and localized symmetrically at the bottom wall of the enclosure. Inclined walls of an equilateral triangular slab placed between hot sources and vertical walls of the enclosure are cooled isothermally at T_c . Length of each heater and height of the triangular slab are chosen $L/4$ and $L/6$, respectively. Other walls of the enclosure are thermally insulated. A uniform magnetic field for three inclination angles $\alpha = 0^\circ, 45^\circ$ and 90° at various Hartmann number ($Ha = 0, 20, 40$ and 80) is applied. The convection flow induced by buoyancy forces is laminar, Newtonian and obeying the Boussinesq approach. Furthermore, radiations effects, induced magnetic field and displacement currents are neglected. To simulate the incompressible thermal problem, SRT-BGK model of LBM is employed.

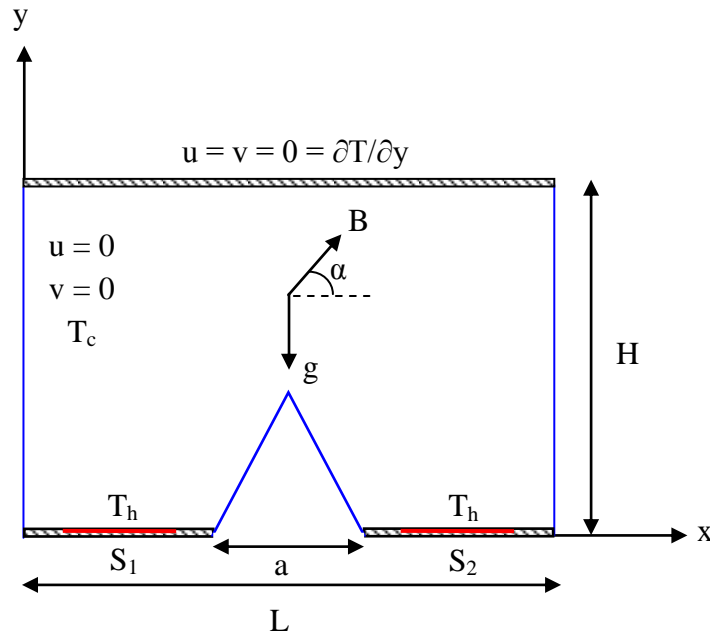


Fig.1 Configuration of the physical problem with boundary conditions

2.2 Lattice Boltzmann method with SRT-BGK and boundary conditions

To compute thermal and dynamic characteristics of the problem, the same code of T. Naffouti et al. [12, 14 and 16] is used with SRT-BGK model of LBM. For this reason, some details will be given in the following section. The fluid domain is discretized in uniform Cartesian cells. The method of LB is based on two populations g and f for temperature and flow, respectively. It is developed by X.He and L.S. Luo [52] with SRT related to the collision operator model of BGK. Discretized LB equations with term force via BGK model is presented for flow and temperature, respectively:

$$f_i(x + c_i \Delta t, t + \Delta t) - f_i(x, t) = -\frac{1}{\tau_f} [f_i(x, t) - f_i^{eq}(x, t)] + (F_{ix} + F_{iy}) \quad (1)$$

$$g_i(x + c_i \Delta t, t + \Delta t) - g_i(x, t) = -\frac{1}{\tau_g} [g_i(x, t) - g_i^{eq}(x, t)] \quad (2)$$

where f_i and g_i are particles distributions functions, f_i^{eq} and g_i^{eq} are equilibrium distributions functions for flow and scalar variable of temperature, respectively. Equilibrium distributions functions related to velocity u , local density ρ and temperature θ of the fluid are defined by:

$$f_i^{eq} = w_i \rho \left[1 + \frac{c_i \cdot u}{c_s^2} + \frac{1}{2} \frac{(c_i \cdot u)^2}{c_s^4} - \frac{1}{2} \frac{u^2}{c_s^2} \right] \quad (3)$$

$$g_i^{eq} = w_i \theta \left[1 + \frac{c_i \cdot u}{c_s^2} \right] \quad (4)$$

For the buoyancy force model, the Boussinesq approach is adopted. Hence, this force is given by the expression:

$$F_{iyg} = 3 w_i g \beta \Delta T \quad (5)$$

The total term force ($F_{ix} + F_{iy}$) applied to flow inside the enclosure is the superposition of buoyancy force with Lorentz force. It is noted by the following expressions:

$$F_{ix} = 3 w_i \rho \frac{Ha^2 \nu}{H^2} (\nu \sin \alpha \cos \alpha - u \sin^2 \alpha) \quad (6)$$

$$F_{iy} = 3 w_i \rho g \beta \Delta T + 3 w_i \rho \frac{Ha^2 \nu}{H^2} (u \sin \alpha \cos \alpha - \nu \cos^2 \alpha) \quad (7)$$

Relaxation time factors of BGK approach for flow and temperature τ_f and τ_g related to kinematic viscosity ν and thermal diffusivity χ are defined as:

$$\tau_f = 3\nu + 0.5 \tag{8}$$

$$\tau_g = 2\chi + 0.5 \tag{9}$$

Speed of the sound, lattice streaming speed, lattice space and lattice time step size equal to unity, are expressed by $c_s = \frac{c}{\sqrt{3}}$, $c = \frac{\Delta x}{\Delta t}$, Δt and Δx , respectively.

Thermal expansion coefficient, temperature difference and gravitational acceleration, macroscopic velocity vector and density are noted by ΔT , g , β , u and ρ , respectively.

To compute the flow dynamic field, D2Q9 model is used (Fig.2) and corresponding weighting factors w_i are given as: $w_0 = \frac{4}{9}$, $w_{1-4} = \frac{1}{9}$, $w_{5-8} = \frac{1}{36}$.

Discrete velocities c_i related to D2Q9 model are given as: $c_0 = (0,0)$, $c_{1-4} = (\pm c, 0)$ and $c_{5-8} = (\pm c, \pm c)$.

The flow temperature is calculated via D2Q4 model (Fig.2) with equal weighting factors $w'_k = 0.25$.

Macroscopic variables of u , ρ and θ are computed by evaluating distributions functions for different directions of nine/four velocity as follows:

$$[\rho, \rho u] = \sum_{i=0}^8 [f_i, c_i f_i] \tag{10}$$

$$[\theta] = \sum_{i=1}^4 [g_i] \tag{11}$$

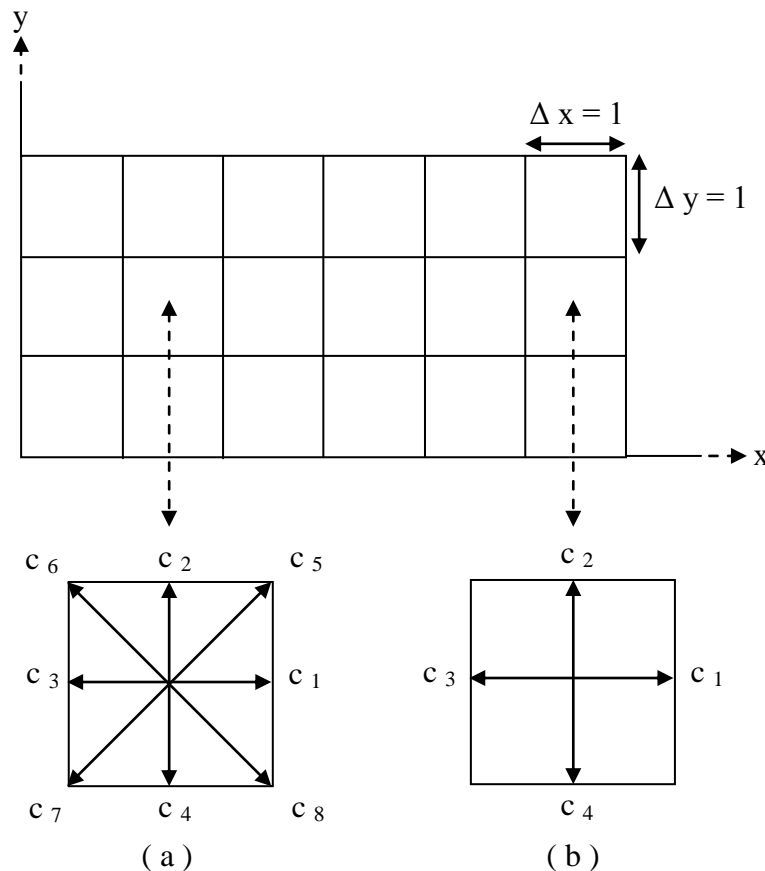


Fig.2 Lattice arrangement: standard models of (a) D2Q9 for flow and (b) D2Q4 for temperature

To simulate the incompressible thermal problem via LBM with SRT-BGK model, the implementation of boundary conditions must be specified. For the Bounce-back boundary conditions on the solid boundaries, D2Q9 model is employed. Boundaries conditions related to distribution functions at north and left inclined walls of the enclosure are given as:

For the north wall:

$$f(4, i, m) = f(2, i, m), f(7, i, m) = f(5, i, m), f(8, i, m) = f(6, i, m) \quad (12)$$

For the left inclined wall of triangular slab:

$$f(2, i, j) = f(4, i, j), f(6, i, j) = f(8, i, j), f(3, i, j) = f(1, i, j) \quad (13)$$

The lattice on the boundary is noted m.

For hot wall heated isothermally at $\theta = 1$, the corresponding boundary condition is defined by the following expression:

$$g(2, i, 0) = 0.5 - g(4, i, 0) \quad (14)$$

For adiabatic bottom wall of the enclosure, the used boundary condition is given as:

$$g(2, i, 0) = g(4, i, 0) \quad (15)$$

Cold boundary conditions applied on vertical and inclined walls of the enclosure are evaluated as:

For left vertical wall:

$$g(1, 0, j) = -g(3, 0, j) \quad (16)$$

For right inclined wall of the triangular slab:

$$g(1, i, j) = -g(3, i, j), g(2, i, j) = -g(4, i, j) \quad (17)$$

2.3 Non-dimensional numbers

For the considered problem in absence/presence magnetic field, the characteristic velocity for free convection is defined by the following expression:

$$U = \sqrt{g \beta \Delta T H} \quad (18)$$

By fixing parameters of Ra, Pr and characteristic velocity (U), kinetic viscosity (ν) and thermal diffusivity (χ) are determined as:

$$\nu = \sqrt{\frac{U^2 H^2}{Ra / Pr}} \quad (19)$$

$$\chi = \frac{\nu}{Pr} \quad (20)$$

Rayleigh number is given as:

$$Ra = \frac{g \beta \Delta T H^3}{\chi \nu} \quad (21)$$

To insure the condition related to an incompressible flow, obtained Mach dimensionless number is less than 0.3.

Mach number is defined as:

$$Ma = \frac{|u|}{c_s} \quad (22)$$

To quantify the Lorentz force intensity, Ha is defined as:

$$Ha = B_0 H \sqrt{\frac{\sigma}{\rho \nu}} \quad (23)$$

where B_0 and σ are the magnetic field magnitude and the electrical conductivity of the fluid, respectively.

The investigation of convective heat transfer inside the enclosure under Lorentz force is a significant parameter quantified by Nusselt number (Nu). Local Nusselt number (Nu_L) and average Nusselt number (Nu) along hot wall are given as:

$$Nu_L = \frac{3\theta_0 - 4\theta_1 + \theta_2}{2} \quad (24)$$

$$Nu = \frac{1}{l} \sum \frac{3\theta_0 - 4\theta_1 + \theta_2}{2} \quad (25)$$

where l is the non-dimensional length of hot wall.

Because of the comparative study of heat transfer between two configurations corresponding to absence or presence of magnetic field, a ratio of Nusselt number Nu^* along hot wall is estimated as follows:

$$Nu^* = \frac{Nu (\neq Ha)}{Nu (Ha=0)} \quad (26)$$

In the present research, the heat transfer is presented vs the magneto convective parameter ε given as:

$$\varepsilon = \frac{Ha^2}{Ra} \quad (27)$$

The significance of this parameter is discussed by Yu et al.[42] about the problem of liquid mercury under various inclination angles of Lorentz force in 2-D cavity. It compares the Lorentz force intensity to buoyancy force. The Lorentz force is weak if ε is close to zero while it is strong for higher ε .

III. RESULTS AND DISCUSSIONS

3.1 Validation of SRT-BGK model of LBM

In the present study, a mesh testing procedure is carried out in order to ensure grid independence of the problem. Fig.3 illustrates the effect of lattices number ranging from 5000 to 125000 on the average Nusselt number along left and right heaters for different Rayleigh number ($10^3 \leq Ra \leq 10^6$) at fixed $Ha = 0$. For $Ra = 10^5$, it is seen that the grid size beyond 80000 lattices is adequate to calculate correctly thermal and dynamic fields of the flow.

To check the accuracy of the proposed SRT-BGK model of the method of LB employed previously [12, 14 and 16], a validation of the numerical approach with results of S.Jani et al.[53] on MHD free convection in a square cavity filled with air and heated from below via VFM is conducted. On Fig.4 is showed a comparison of streamlines and isotherms of the flow for a fixed $Ra = 10^5$ in the absence and presence of Lorentz force corresponding to $Ha = 0$ and $Ha = 50$, respectively. It is shown an excellent agreement between present results and those of S.Jani et al.[53]. Table.1 illustrates a comparison of the average Nusselt number calculates along hot wall for both computational methods versus Ra and Ha . Based on numerical data of Table.1, an excellent agreement is concluded. Consequently, this successful validation proves that the method of LB with SRT-BGK model is a vital tool to resolve problems of free convection under a Lorentz force.

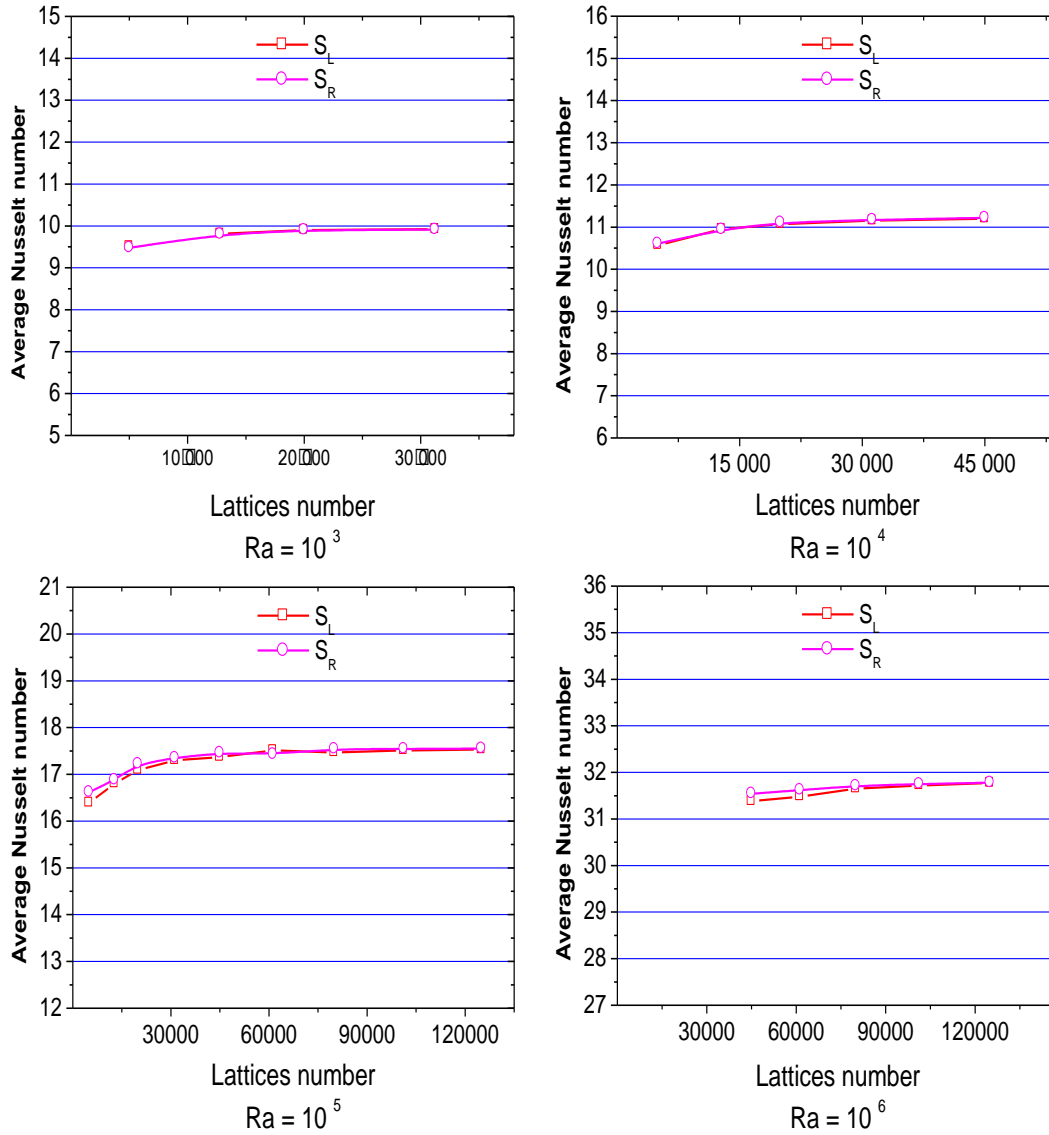


Fig.3 Lattices number effect on the average Nusselt number along left and right hot walls (S_L and S_R) versus Rayleigh number for Ha = 0

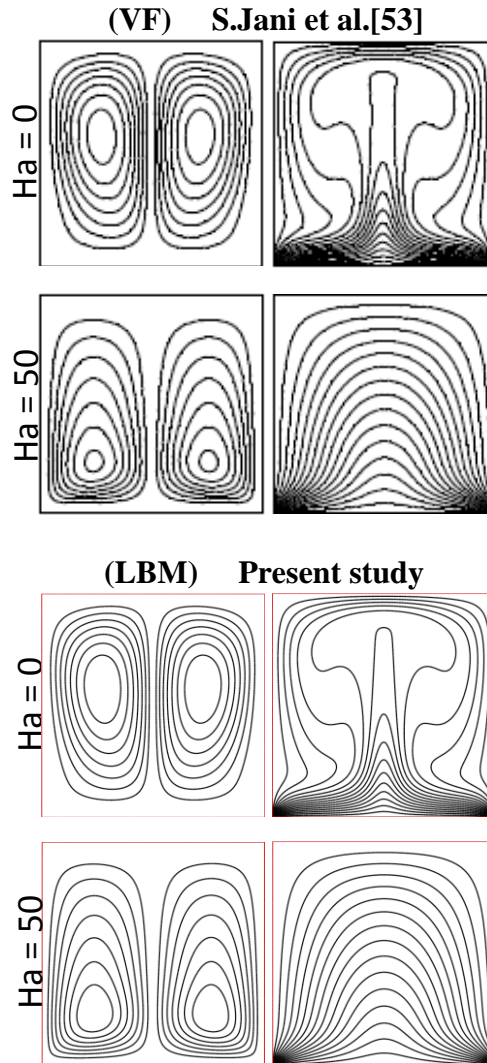


Fig.4 Comparison between present results via SRT-BGK model of LBM with those of S.Jani et al.[53] using VF method: streamlines (left) and isotherms (right)

	<u>Present results via SRT model of LB method</u>			<u>Results of S.Jani et al. [53] via VF method</u>		
	Ha = 0	Ha = 50	Ha = 100	Ha = 0	Ha = 50	Ha = 100
Ra = 10³ (161*161)	7.37	7.36	7.36	7.39	7.37	7.34
Ra = 10⁴ (171*171)	8.17	7.37	7.36	8.19	7.41	7.37
Ra = 10⁵ (181*181)	10.46	7.97	7.43	10.41	8.03	7.50
Ra = 10⁶ (201*201)	14.83	13.31	10.68	14.78	13.21	10.62

Table.1 Comparative study of present results with those of S.jani et al.[53] on MHD free convection in a 2-D enclosure heated from below for Pr = 0.7

3.2 Global view of the flow in the absence of magnetic field

Contour maps of isotherms and streamlines of the flow for different Rayleigh number for a fixed $Ha = 0$ corresponding to case of the absence of magnetic field are depicted in Fig.5. It is found symmetrical behaviors of temperature and buoyant convection flow fields about the mid-length of the enclosure owing to symmetrical boundary conditions of the problem. As it can be seen from the figure, each thermal plume generated by one heater is asymmetrically supplied in fresh air from neighboring vertical and inclined cold walls. Consequently, the dynamic structure of the resulting flow of two thermal plumes is described by four cells with clockwise and anticlockwise rotations and for different sizes. For smaller Rayleigh number

($Ra = 10^3$), the circulation of the flow is so feeble and isotherms of thermal plumes deviate slightly toward the central region of the enclosure owing to the dominance of viscous forces over the buoyancy force. Consequently, the heat transfer is dominated by conduction mode and the interaction between thermal plumes is negligible. The growth of Ra causes an increase of the degree of stratification of isotherms close to cold walls and each heater causing an increase of thermal field intensity and an acceleration of all cells of the resulting flow inside the enclosure. Furthermore, recirculation and size of cell in the vicinity of vertical cold wall increase as increasing Ra due to an intensification of entrainment fresh air in the region between hot source and this one. Therefore, these findings prove that the convection which becomes dominant over the conduction enhances the communication between thermal plumes as growing Ra .

3.3 Global view of the flow under magnetic field

Next attention is focused on the effect of a uniform magnetic field with three directions on thermal and dynamic structures of the resulting flow at $Ra = 10^5$. On Figs.6-8 are illustrated isotherms and streamlines of the flow versus Hartmann number ranging from 20 to 80 for inclination angle $\alpha = 0^\circ$, $\alpha = 45^\circ$ and $\alpha = 90^\circ$. Global view of the flow proves that temperature and velocity distributions are strongly affected by strength and direction of magnetic field. From Fig.6 related to horizontal magnetic field at $\alpha = 0^\circ$, it is found a significant attenuation of the intensity of symmetrical thermal and dynamic fields inside the enclosure and consequently the interaction between thermal plumes becomes weaker as increasing Hartmann number. Indeed, the existence of magnetizing force over buoyancy force conducts to stabilize the flow causing the suppression of convection in particular for the higher Hartmann number at 80. For the case of inclined direction of magnetic field corresponding to $\alpha = 45^\circ$, Fig.7 shows that the dissymmetric flow is described usually by four cells with different sizes. Plots of isotherms and streamlines show a decrease of the degree of thermal stratification and a significant deceleration of the flow for a growth of magnetic field strength. This result proves that the buoyancy force becomes weaker over magnetizing force thus indicating the convection mode is suppressed and the heat transfer is owing to conduction. Furthermore, a strong deviation of the left thermal plume to right vertical cold wall is observed as increasing Ha due to the decrease of the entrainment phenomenon of fresh air close to this one. It is related to the effect of inclined direction of magnetic field on resulting flow. These conclusions prove that the magnetic field can destroy the communication between thermal plumes above the triangular slab especially for $Ha = 80$. For the case of vertical magnetic field ($\alpha = 90^\circ$), Fig.8 the flow is characterized by symmetrical temperature and velocity distributions with a decrease of these parameters as increasing Hartmann number. For higher strength of magnetic field at $Ha = 80$, the flow is stabilized and the interaction of thermal plumes is so feeble above the triangular slab due to the weakening of the convection mode inside the enclosure.

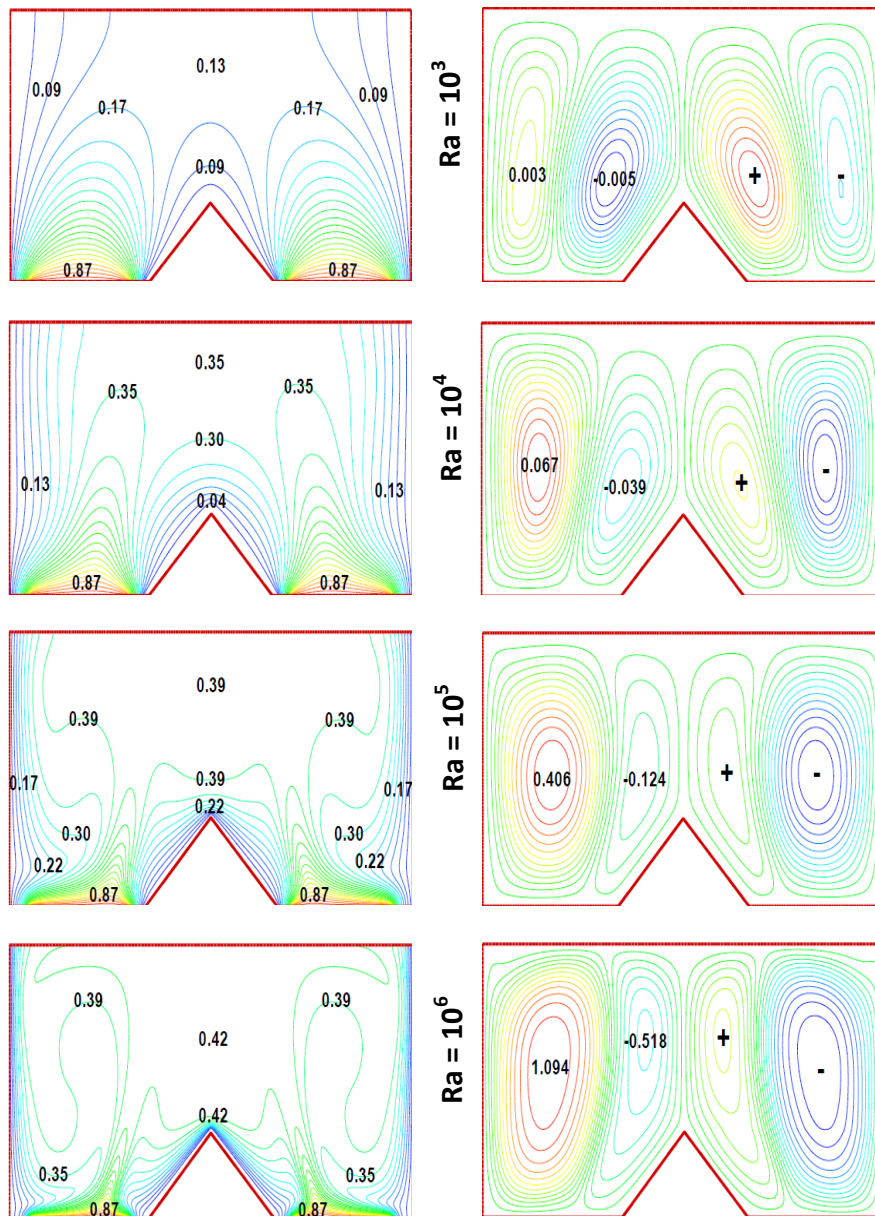


Fig.5 Isotherms (left) and streamlines (right) of the flow versus Ra for Ha = 0

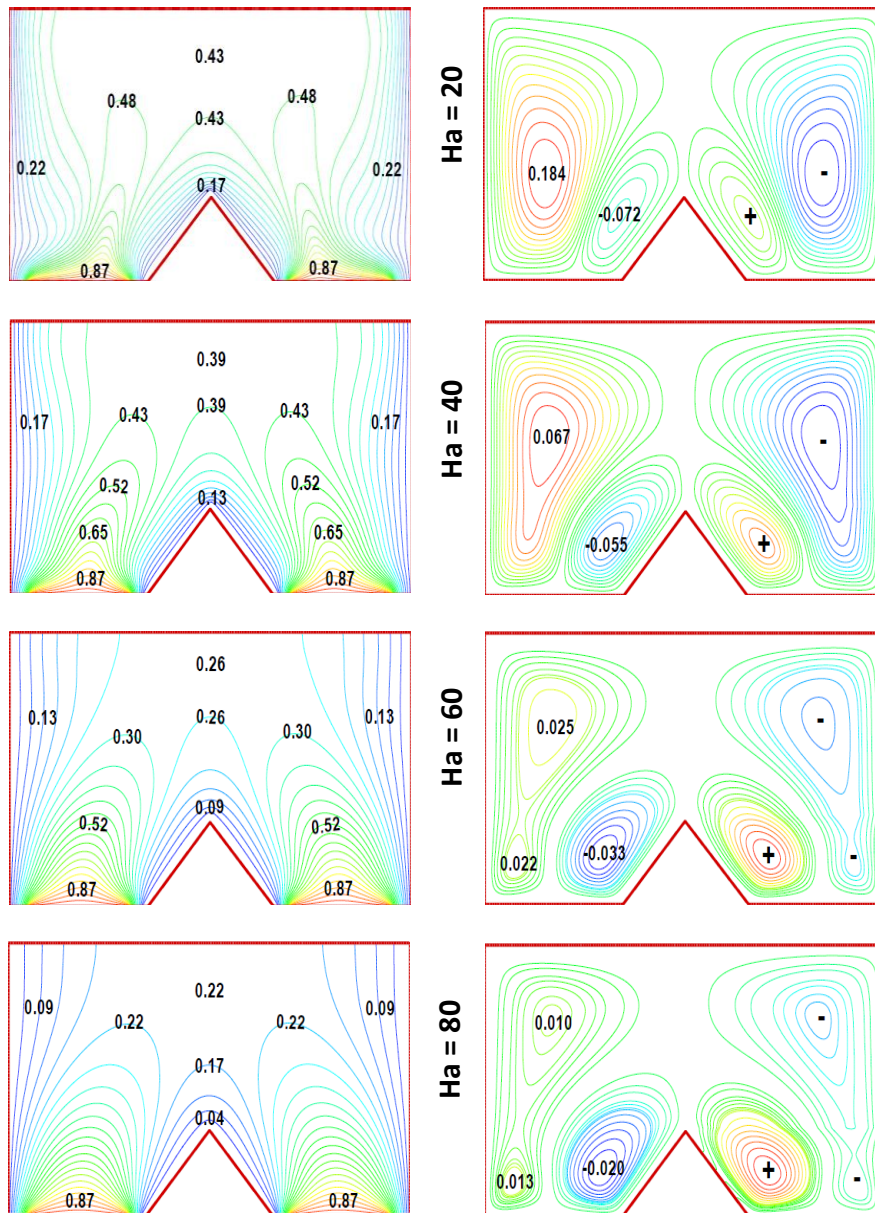


Fig.6 Isotherms (left) and streamlines (right) of the flow versus Ha for $Ra = 10^5$ and horizontal magnetic field

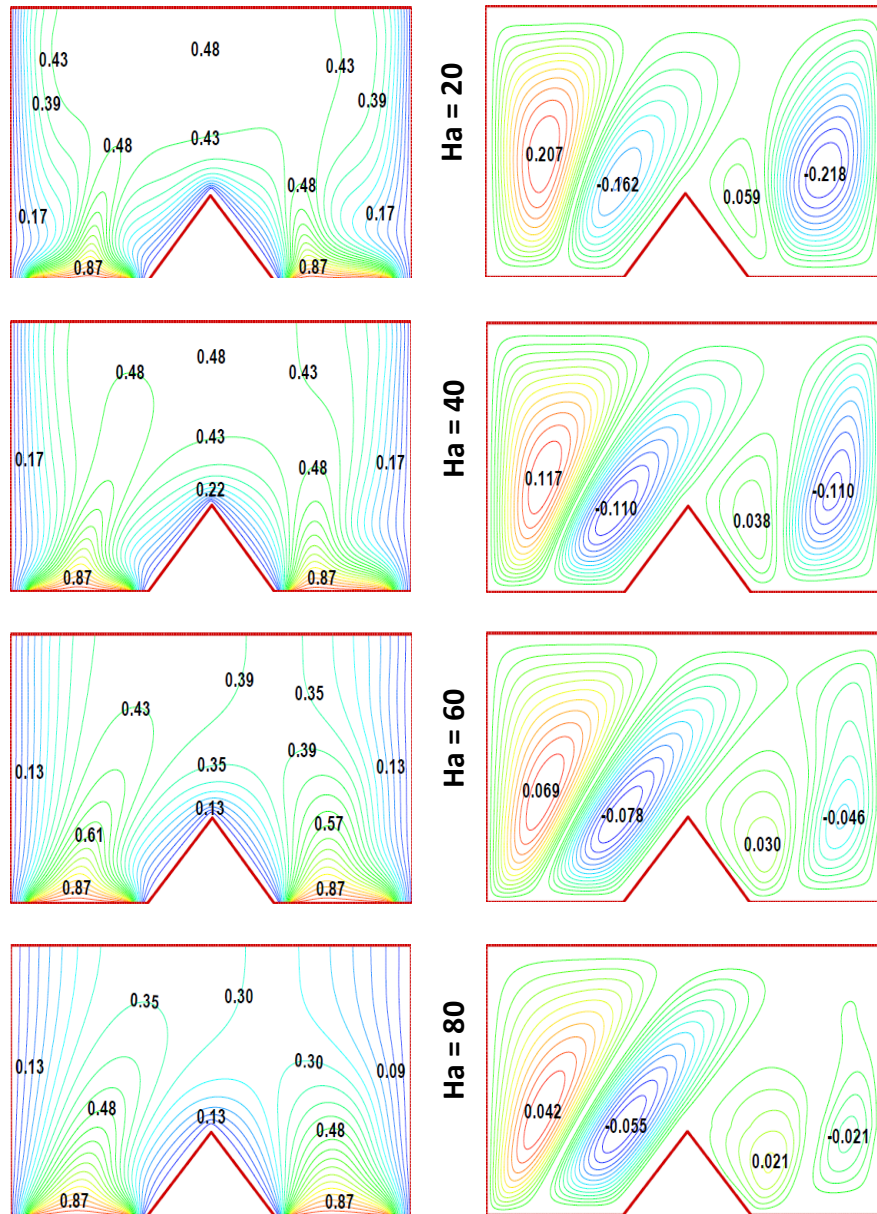


Fig.7 Isotherms (left) and streamlines (right) of the flow versus Ha for $Ra = 10^5$ and inclined magnetic field

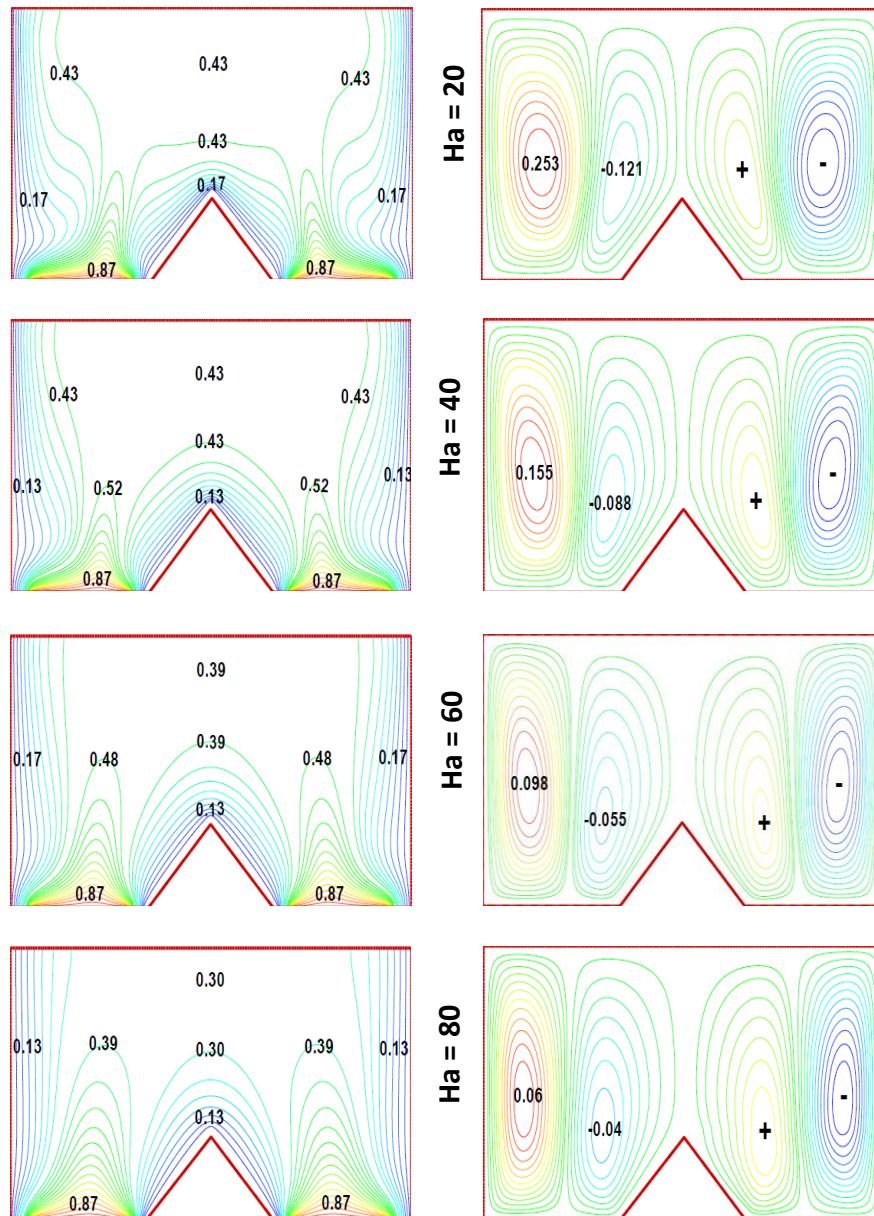


Fig.8 Isotherms (left) and streamlines (right) of the flow versus Ha for $Ra = 10^5$ and vertical magnetic field

IV. EFFECT OF MAGNETIC FIELD ON TEMPERATURE AND VERTICAL COMPONENT VELOCITY OF THE FLOW

4.1 Vertical evolution of temperature and velocity

Effects of three directions of a magnetic field on temperature and velocity of the flow at mid-length of the enclosure is presented in Fig.9 with different Hartmann number for $Ra = 10^5$. As increasing Ha from 20 to 80, profiles of temperature and velocity show an attenuation of these parameters above the triangular slab in order to reach values about 0.2 and zero, respectively. For the case of a horizontal magnetic field corresponding to $\alpha = 0$, it is clear that values of temperature are weaker in particularly for $Ha = 80$. Then, it is concluded that an intense magnetic field can suppress the convection causing a stabilization of the resulting flow. Consequently, the interaction between thermal plumes is destroyed in the presence of a magnetic field in particularly for a horizontal direction related to $\alpha = 0$. These conclusions can consolidate previous results presented by global views of isotherms and streamlines given in Fig.6.

Fig.10 delineates the variation of maximums temperature and velocity at mid-length of the enclosure for different Ha and directions of magnetic field at $Ra = 10^5$. As it can be seen from the figure, practically the same behavior is obtained for each parameter versus angle inclination of magnetic field. The growth of the magnetic field strength from $Ha = 0$ to 80 conducts to an attenuation of temperature and velocity of the resulting

flow in the central region of the enclosure causing a weakening of the communication between thermal plumes above the active triangle slab.

4.2 Transversal distribution of temperature and vertical component velocity

Plots of the transversal distribution of temperature and velocity as a function of Ha for three sections with various directions of the magnetic field at $Ra = 10^5$ are given in Figs.11-13. Profiles evolutions prove that thermal and dynamic fields of the resulting flow are strongly affected by two pertinent parameters of Hartmann number and angle inclination of the magnetic field.

For the case of a horizontal magnetic field ($\alpha = 0^\circ$), Fig.11 shows a considerable variation of the temperature and velocity as moving away from active heaters toward upper adiabatic wall of the enclosure. For the first section close to hot sources ($y = 0.25$), thermal and dynamic gradients are more intense on both sides of the triangular slab due to the dominance of thermal plume with a significant recirculation in particularly for $Ha = 0$. Negative values of the velocity are related to existence of fresh air near cold vertical walls in order to supply heaters. In the vicinity of the triangular slab, lower values of temperature and velocity are related to existence of fresh air with a feeble circulation of the flow. The increase of Ha causes a displacement of the temperature maximum from vertical axis of the enclosure at $x = L/2$ with a deceleration of the flow thus reflects a symmetrical deviation of both thermal plumes to vertical cold walls. Moreover, an intensification of the magnetizing force conducts to a strong attraction of one thermal plume to vertical wall of the enclosure and consequently the communication between thermal plumes is weaker. For the second section at mid-height of the enclosure ($y = 0.5$) and for different Ha , the temperature increases above the triangular slab while it decreases on both sides of this one. In addition, an attenuation of the temperature is observed with the growth of Ha . For the section at $y = 0.75$, the temperature remains practically constant thus indicating a homogenization of the fluid in the upper part of the enclosure. With increasing Ha in this region, it is found a decrease of temperature and velocity about to 0.2 and zero and consequently a stabilization of the flow is obtained for higher Ha .

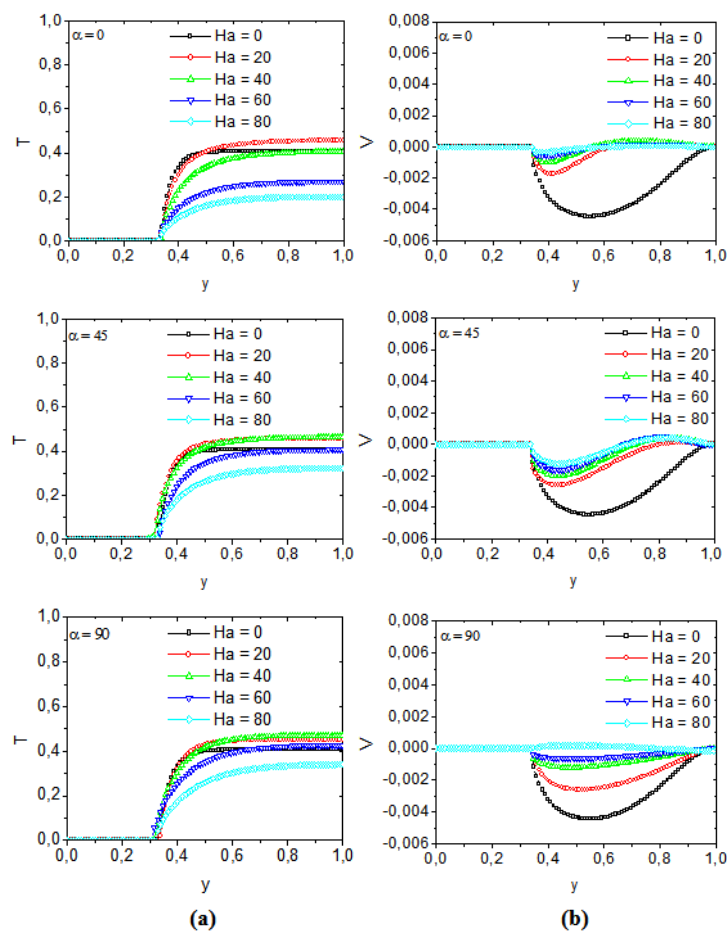


Fig.9 Vertical evolution of: (a) temperature and (b) vertical component velocity of the flow versus Ha at mid-length of the enclosure for various inclinations of magnetic field at $Ra = 10^5$

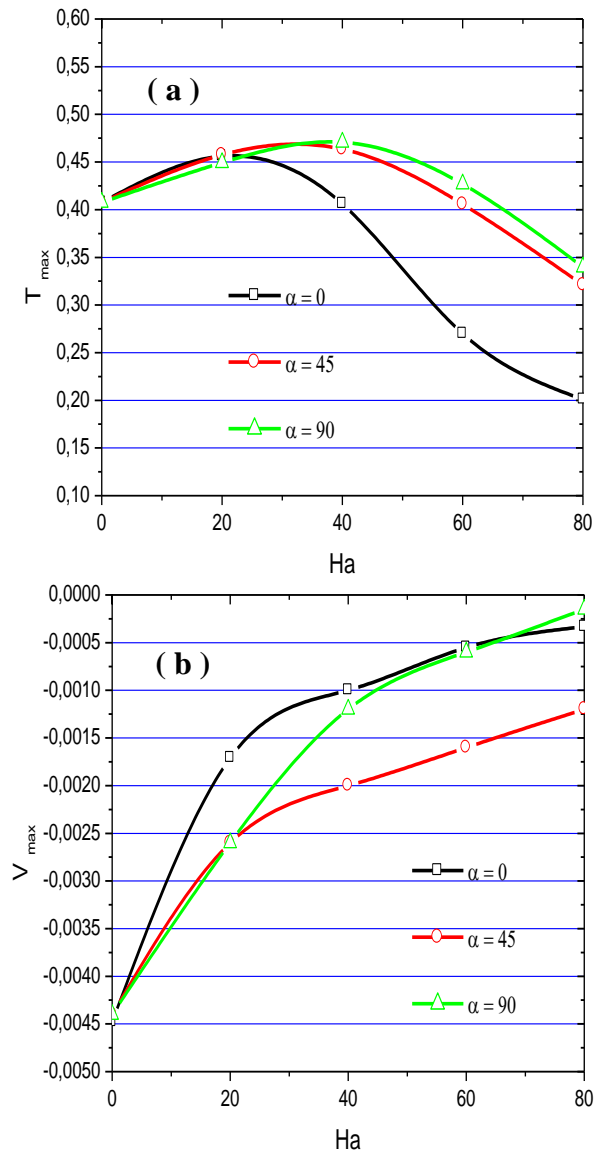


Fig.10 Evolution of maximums: (a) temperature and (b) vertical component velocity of the flow at mid length of the enclosure versus Ha for various inclinations of magnetic field at $Ra = 10^5$

Concerning the second case of an inclined magnetic field ($\alpha = 45^\circ$) related to Fig.12, thermal and dynamic profiles are asymmetrical owing to the strong effect of the magnetizing force with inclined direction over vertical buoyancy force. As increasing the magnetic field strength ($0 \leq Ha \leq 80$), it is shown a deviation of plots related to the left thermal plume toward vertical axis at mid-length of the enclosure. For all sections ($y = 0.25, 0.5$ and 0.75), a deceleration of the resulting flow is detected with a growth of Ha thus translating a stabilization of the flow for higher Ha in particularly at 80. Consequently, the convective mode is more suppressed with increasing Hartmann number for an inclined magnetic field at 45° . For the third case of a vertical magnetic field ($\alpha = 90^\circ$), symmetrical distributions of temperature and velocity are showed on Fig.13 due to the superposition of a horizontal magnetizing force with the buoyancy force. From figures, it is found the same behavior of the resulting flow compared to that of the case of horizontal magnetic field with a slight intensification of thermal and dynamic field. This result proves that the interaction of thermal plumes is not negligible for the case of a vertical magnetic field and consequently the convection is not completely suppressed.

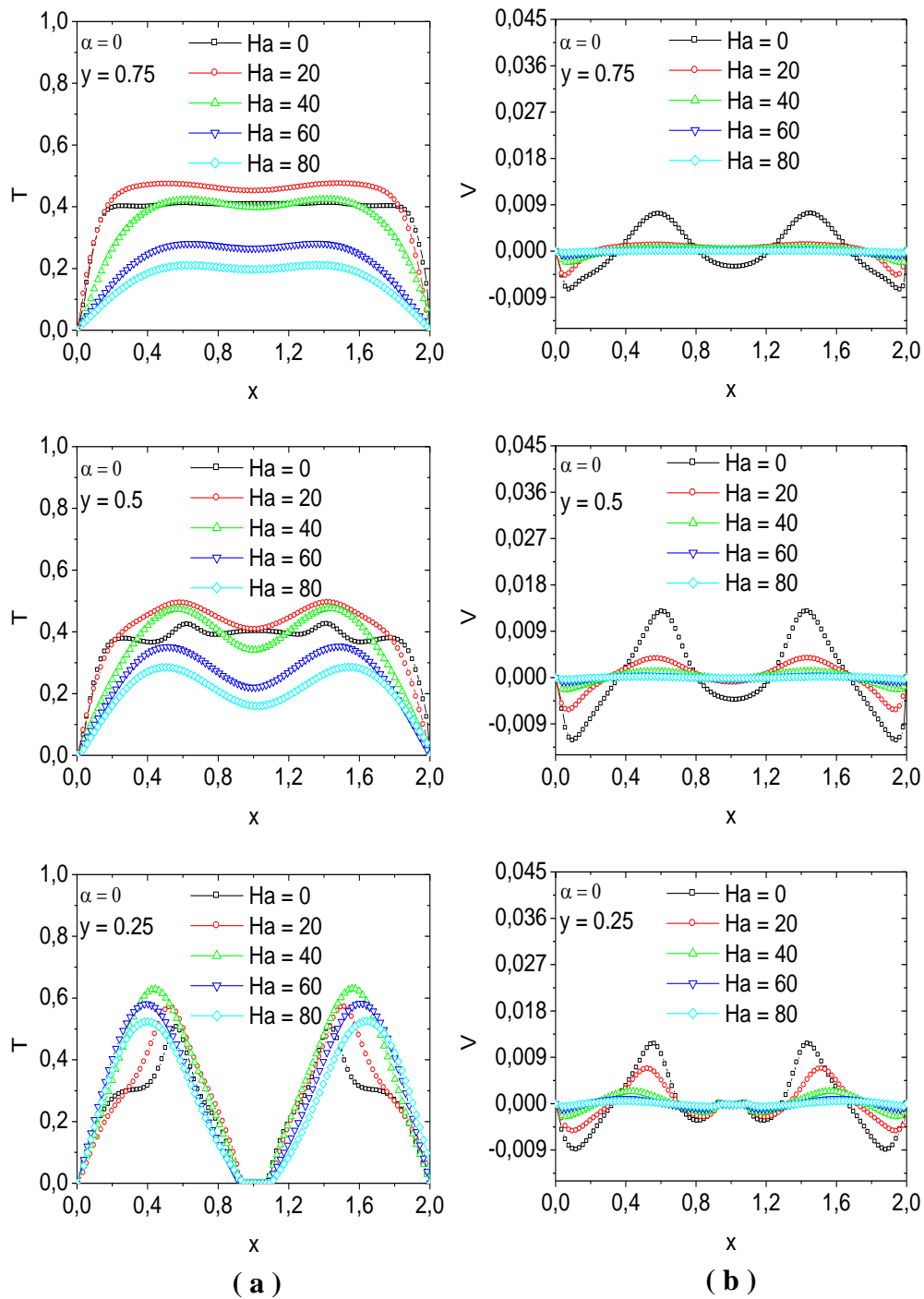


Fig.11 Transversal distribution of: (a) temperature and (b) vertical component velocity of the flow versus Ha for three sections with horizontal magnetic field at $Ra = 10^5$

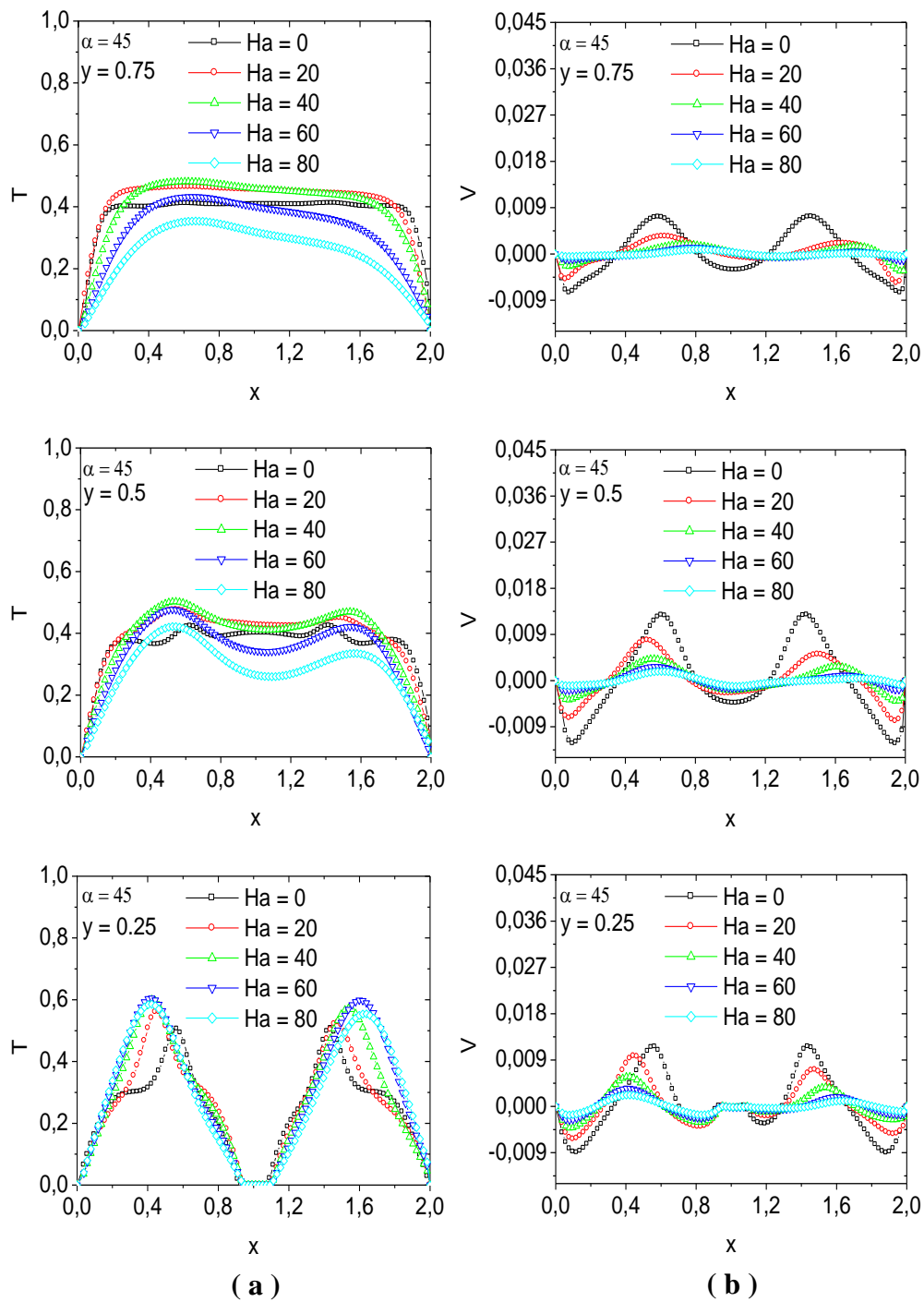


Fig.12 Transversal distribution of: (a) temperature and (b) vertical component velocity of the flow versus Ha for three sections with inclined magnetic field at $Ra = 10^5$

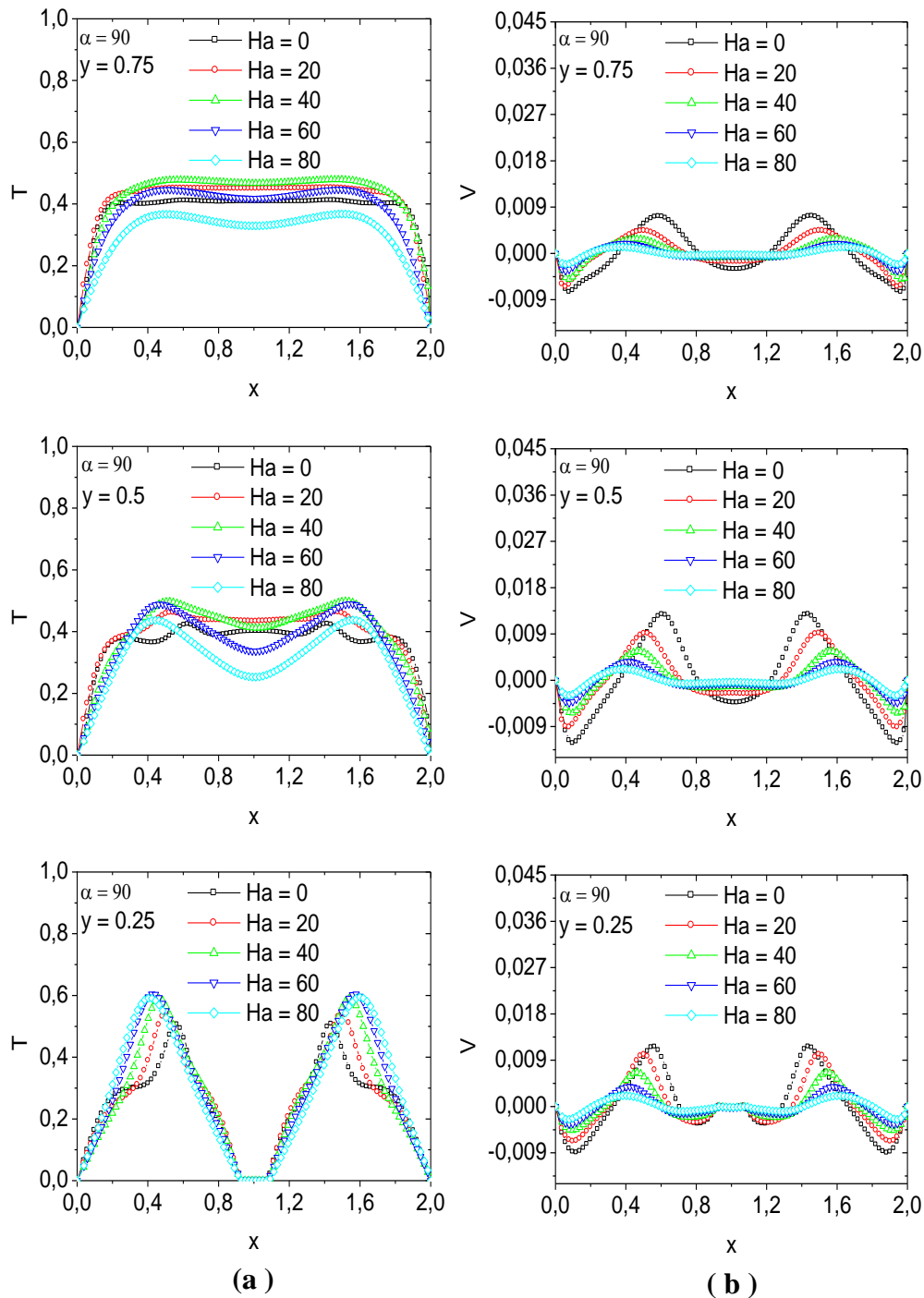


Fig.13 Transversal distribution of: (a) temperature and (b) vertical component velocity of the flow versus Ha for three sections with vertical magnetic field at $Ra = 10^5$

V. EFFECT OF MAGNETIC FIELD ON FLOW HEAT TRANSFER

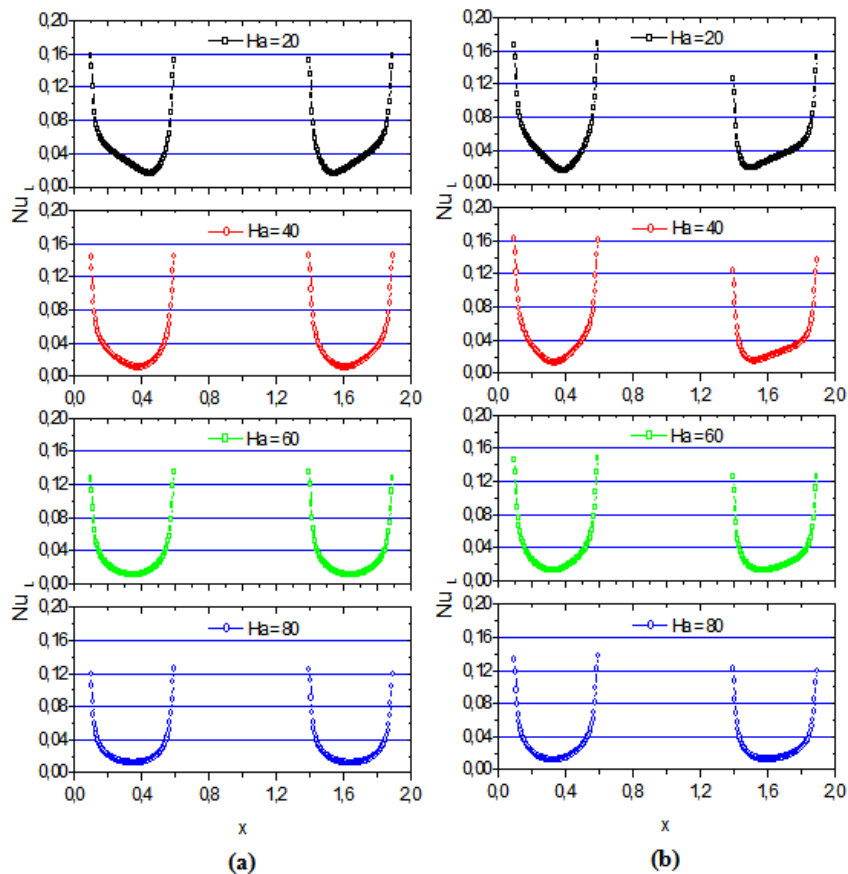
5.1 Variation of local Nusselt number

Next concentration is focused on the investigation of heat transfer of the resulting flow within enclosure. It is quantified by the local Nusselt number (Nu_L) along both hot sources S_1 and S_2 in order to better understanding the physics of the buoyancy convection under various directions and strength of magnetic field. For a fixed Ra at 10^5 , the variation of Nu_L along each heater versus strength and direction of magnetic field is illustrated on Fig.14. As it can be seen from plots, the heat transfer strongly depends with different Ha and angle

inclination of the magnetic field. For the case of a horizontal magnetic field ($\alpha = 0^\circ$) corresponding to vertical magnetizing force (Fig.14.a), Nu_L is more important on sides of each hot source owing to the existence of strong thermal gradients. As increasing Ha from 20 to 80, it is clear a reduction of heat transfer about 20% on heaters sides thus indicating the decrease of the convection effect under the intensification of magnetizing force over buoyancy force. For the case of inclined direction of magnetic field (Fig.14.b), it is found an attenuation of heat transfer rate with the growth of Ha . Moreover, the figure shows that the heat transfer is described by an asymmetrical behavior inside the enclosure. It is more important along left source S_1 than that second source S_2 for various Ha due to the dominance of the convection over conduction at the left region of the enclosure. Fig.14.c related to case of vertical magnetic field demonstrates a decrease of heat transfer on each heater sides about 15% as increasing Ha from 20 to 80. Compared to case of horizontal magnetic field where $\alpha = 0^\circ$, the convective heat transfer for a vertical magnetic field corresponding to $\alpha = 90^\circ$ is stronger about 5%.

5.2 Variation of the ratio Nusselt number

On Fig.15 is depicted the evolution of the ratio Nusselt number (Nu^*) along each heater (S_1 and S_2) versus the magneto-convective parameter ϵ for various angle inclination of magnetic field α at $Ra = 10^5$. For various directions of the magnetic field, it is found that increasing ϵ decrease the Nu^* owing to a weak effect of buoyancy force over magnetizing force. Consequently, the contribution of heat transfer by convection becomes weaker in particularly for higher Ha while the conduction mode is dominant. From figure, the maximum heat transfer is detected for the case of the vertical magnetic field (view Fig.15.c) while it is weaker for the case of horizontal magnetic field (view Fig.15.a). Concerning the case of an inclined magnetic field corresponding to $\alpha = 45^\circ$, the ratio of Nusselt number along left heater S_1 is more significant than that of the right heater S_2 owing to the inclined direction of magnetic field.



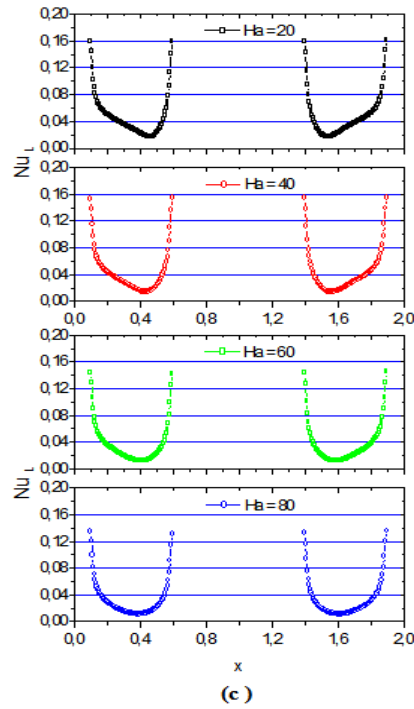


Fig.14 Variation of the local Nusselt number along each heater versus Ha for: (a) horizontal magnetic field ($\alpha = 0^\circ$), (b) inclined magnetic field ($\alpha = 45^\circ$) and (c) vertical magnetic field ($\alpha = 90^\circ$) at $Ra = 10^5$

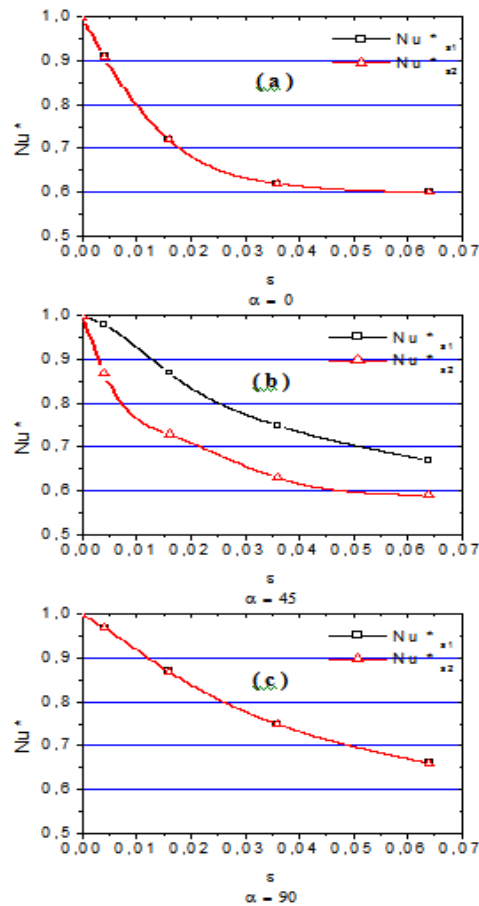


Fig.15 Variation of Nusselt number along each heater S_1 and S_2 for various magneto convective parameter ϵ and angle inclination of magnetic field α at $Ra = 10^5$

VI. CONCLUSION

Effects of intensity and direction of a uniform magnetic field on free convection generated from two heaters placed at the bottom wall of a rectangular horizontal enclosure containing an active triangle slab localized at the center of this one. Numerical simulations are performed with SRT-BGK model of LBM. Firstly, the problem is studied for the case in the absence of a Lorentz force at various $Ra = 10^3$ to 10^6 . Secondly, the study is discussed for the case in the presence of a Lorentz force with a fixed Rayleigh number at 10^5 . For this case, three directions of the magnetic field $\alpha = 0^\circ, 45^\circ$ and 90° at different $Ha = 0$ to 80 are applied to the problem. It is concluded that the successful validation of results via SRT-BGK model of LBM with previous investigations proves that this numerical approach is a vital tool to simulate buoyancy convection problem under the Lorentz force. For the $Ha = 0$, symmetrical isotherms and streamlines demonstrate that the increase of Ra conducts to an intensification of the convection over the conduction causing a stronger interaction between thermal plumes above the triangular slab. In the presence of magnetic field, thermal and dynamic fields as well as heat transfer are strongly affected by pertinent parameters of Ha and angle inclination α . The growth of Ha shows an intensification of the magnetizing force over buoyancy force with various inclination angles α . Consequently, it conducts to a brake the flow and to neglect the convection in particularly for the higher Ha . Furthermore, it is found that the communication of thermal plumes can be totally destroyed via a horizontal magnetic field for higher Ha . For $Ra = 10^5$, optimization of heat transfer proves that the minimum of this one is obtained for horizontal magnetic field while it is stronger for the case of a vertical magnetic field.

Nomenclature

B_0	magnitude of magnetic field
c_s	lattice sound speed
c_i	discrete lattice velocity
f_i	discrete distribution function for the density
g_i	discrete distribution function for the temperature
g	gravity field
H	dimensionless height of the enclosure
Ha	Hartmann number
L	dimensionless length of the enclosure
Nu_L	local Nusselt number along heater
Nu	average Nusselt number along heater
Nu^*	ratio Nusselt number along heater
Pr	Prandtl number
Ra	Rayleigh number
S_1	left heater
S_2	right heater
T_h	temperature of heater
T_c	temperature of cold wall
U	velocity vector (u, v)
X	lattice node in (x, y) coordinates
Δx	lattice spacing units ($=\Delta y$)
ΔT	temperature gradient
Δt	time step
α	inclination angle
w_i	weighting factors for f_i
w_i	weighting factors for g_i

Greek symbols

β	thermal expansion coefficient
θ	dimensionless temperature field
ε	magneto convective parameter
τ_f	relaxation time for f_i
τ_g	relaxation time for g_i
ρ	fluid density
ν	kinetic viscosity
χ	thermal diffusivity
σ	electrical conductivity

Subscripts

- c cold
h hot
eq equilibrium part
i discrete speed directions (i=0, ..., 8)

REFERENCES

- [1]. Jaluria, Y., Natural Convection Cooling of Electronic Equipment. In Natural convection: Fundamental and Applications (Edited by S. Kakac et al.), pp. 961-986, (1985).
- [2]. Incropera, F. P., Convection Heat Transfer in Electronic Equipment Cooling, ASME, Journal of Heat Transfer, Vol. 110, pp. 1097-1111, (1988).
- [3]. Prasad, V., Keyhani, M. and Shen, R., Free Convection in a Discretely Heated Vertical Enclosure: Effects of Prandtl Number and Cavity Size, ASME, Journal of Electronic Packaging, Vol. 112, pp. 63-74, (1990).
- [4]. G.P. Peterson and A. Ortega, Thermal control of electronic equipment and devices, Advances in Heat Transfer, vol. 20, pp: 181-214, (1990).
- [5]. Selamat, E. E., Arpacı, V. S. and Borgnakke, C., Simulation of Laminar Buoyancy Driven Flows in an Enclosure, Numerical Heat Transfer, Vol. 22, pp. 401-420, (1992)
- [6]. S.J. Kim and S.W. Lee, Air cooling Technology for Electronic Equipment, CRC Pres, Boca Raton, LA, (1996).
- [7]. Skouta, A., Randriazanamparant, M.A. and Dagueuet, M.L, Numerical Study of Two-Dimensional Transient Convection in an Air Filled Square Enclosure, Tilted In Relation To The Horizontal Plane, Heated from Two Opposite Sides, International Journal of Therm.Sci.,40, pp. 352-365, (2001).
- [8]. Costa, V.A., Oliviera, M. and Sousa, "Control Of Laminar Natural Convection In differentially Heated Square Enclosure Using Solid Inserts At The Corner", International Journal of Heat and Mass Transfer, Vol. 46, pp. 3529-3537, (2003).
- [9]. B. Calgagni, F. Marsili, M. Paroncini, Natural convective heat transfer in square enclosures heated from below, Appl. Therm. Eng. 25, pp. 2522-2531, (2005).
- [10]. Altac, Z. and Konrat, S., "Natural Convection Heat Transfer From A thin Horizontal Isothermal Plate in Air-Filled Rectangular Enclosure", J. of Thermal Science and Technology, 29, No. 1, pp. 55-56, (2009).
- [11]. T. Naffouti and R. Djebali, Natural convection flow and heat transfer in square enclosure asymmetrically heated from below: A lattice Boltzmann comprehensive study, Computer Modeling in Engineering and Sciences, 88 (3), pp. 211-227, (2012).
- [12]. T. Naffouti, J. Zinoubi and R. Ben Maad, Lattice Boltzmann Analysis of 2-D Natural Convection Flow and Heat Transfer within Square Enclosure including an Isothermal Hot Block, International Journal of Thermal Technologies, vol.3, No.4 (2013).
- [13]. R. F. Elsayed, M. K. Elriedy, E. A. Elkady, Mustafa Ali, Natural Convection Heat Transfer Optimization From A Horizontal Finned Tube, Journal of Multidisciplinary Engineering Science and Technology, vol. 3, Issue 12, pp. 6141-6150, (2016).
- [14]. T. Naffouti, J. Zinoubi, N. A. Che Sidik and R. B. Maad, Applied Thermal Lattice Boltzmann Model for Fluid Flow of Free Convection in 2-D Enclosure with Localized Two Active Blocks: Heat Transfer Optimization, Journal of Applied Fluid Mechanics, vol. 9, No. 1, pp. 419-430, (2016).
- [15]. Ahmed Kadari, Nord-Eddine Sad Chemloul and Said Mekroussi, Numerical Investigation of Laminar Natural Convection in a Square Cavity With Wavy Wall and Horizontal Fin Attached to the Hot Wall, *J. Heat Transfer* 140(7), pp. 1-15, (2018).
- [16]. Taoufik Naffouti, LamiaThamri, Awatef Naffouti and Jamil Zinoubi, Optimization of Convective Heat Transfer from Two Heating Generators into Horizontal Enclosure Including A Discrete Obstacle: A Lattice Boltzmann Comprehensive Investigation, Journal of Applied Fluid Mechanics, Vol. 11, No. 5, pp. 1277-1286, (2018).
- [17]. C. Vives, C. Perry, Effects of magnetically damped convection during the controlled solidification of metals and alloys. International Journal of Heat and Mass Transfer, 30, pp. 479-496, (1987).
- [18]. H. Ozoe, E. Maruo, Magnetic and gravitational natural convection of melted silicone two-dimensional numerical computations for the rate of heat transfer. JSME 30, pp. 774-784, (1987).
- [19]. H. Ozoe, K. Okada, The effect of the direction of the external magnetic field on the three-dimensional natural convection flow in a cubical enclosure. International Journal of Heat and Mass Transfer 32, pp. 1939-1954, (1989).
- [20]. R.W. Series, D.T.J. Hurlle, The use of magnetic fields in semiconductor crystal growth. Journal of Crystal Growth 133, pp. 305-328, (1991).
- [21]. J.P. Garandet, T. Alboussiére, M. Moreau, Buoyancy driven convection in a rectangular enclosure with a transverse magnetic field. International Journal of Heat and Mass Transfer 35, pp. 741-748, (1992).
- [22]. M. Venkatachalappa, C.K. Subbaraya, Natural convection in a rectangular enclosure in the presence of magnetic field with uniform heat flux from side walls. Acta Mechanica 96, pp. 13-26, (1993).
- [23]. N. Rudraiah, R.M. Barron, M. Venkatachalappa, C.K. Subbaraya, Effect of magnetic field on free convection in a rectangular enclosure. International Journal of Engineering Science 33, pp. 1075-1084, (1995).
- [24]. S. Alchaar, P. Vasseur, E. Bilgen, Natural convection heat transfer in a rectangular enclosure with transverse magnetic field. Journal of Heat Transfer e Transactions of the ASME 117, pp. 668-673, (1995).
- [25]. T. Tagawa, H. Ozoe, Enhancement of heat transfer rate by application of a static magnetic field during natural convection of a liquid metal in a cube, ASME J. Heat Transfer 119, pp. 265-271, (1997).
- [26]. N.M. Al-Najem, K.M. Khanafer, M.M. El-Rafae, Numerical study of laminar natural convection in tilted enclosure with transverse magnetic field, Int. J. Numer. Meth. Heat Fluid Flow 8, pp. 651-672, (1998).
- [27]. A.Y. Gelfgat, P.Z. Bar-Yoseph, The effect of an external magnetic field on oscillatory instability of convective flows in a rectangular cavity, Phys. Fluids 13 (8), pp. 2269-2278, (2001).
- [28]. J.P. Garandet, T. Alboussiére, R. Moreau, Buoyancy driven convection in a rectangular enclosure with a transverse magnetic field, Int. J. Heat Mass Transfer 35 (4), pp. 741-748, (1992).
- [29]. T. Tagawa, R. Shigemitsu, and H. Ozoe, "Magnetizing force modeled and numerically solved for natural convection of air in a cubic enclosure: effect of the direction of the magnetic field," International Journal of Heat and Mass Transfer, vol. 45, no. 2, pp. 267-277, (2002).
- [30]. M. Akamatsu, M.Higano, Y. Takahashi, and H.Ozoe, "Numerical computation on the control of aerial flow by the magnetizing force in gravitational and non gravitational fields," Numerical Heat Transfer A: Applications, vol. 43, no. 1, pp. 9-29, (2003).
- [31]. I.E. Sarris, S.C. Kakarantzas, A.P. Grecos, N.S. Vlachos, MHD natural convection in a laterally and volumetrically heated square cavity, International Journal of Heat and Mass Transfer 48, pp. 3443-3453, (2005).

- [32]. Sarris, I.E., Zikos, G.K., Grecos, A.P., Vlachos, N.S., On the limits of validity of the low magnetic Reynolds number approximation in MHD natural-convection heat transfer. *Numer. Heat Transf. B: Fundam.* 50 (2), pp. 157–180, (2006).
- [33]. T. Bednarz, E. Fornalik, H. Ozoe, J. S. Szmyd, J. C. Patterson, and C. Lei, "Influence of a horizontal magnetic field on the natural convection of paramagnetic fluid in a cube heated and cooled from two vertical side walls," *International Journal of Thermal Sciences*, vol. 47, no. 6, pp. 668–679, (2008).
- [34]. P. Kandaswamy, S. Malliga Sundari, N. Nithyadevi, Magnetoconvection in an enclosure with partially active vertical walls, *Int. J. Heat Mass Transfer* 51, pp. 1946–1954, (2008).
- [35]. M. Pirmohammadi, M. Ghassemi, G.A. Sheikhzadeh, Effect of magnetic field on buoyancy driven convection in differentially heated square cavity, *IEEE Trans. Magn.* 45, pp. 407–411, (2009).
- [36]. T. P. Bednarz, C. Lei, J. C. Patterson, and H. Ozoe, "Effects of a transverse, horizontal magnetic field on natural convection of a paramagnetic fluid in a cube," *International Journal of Thermal Sciences*, vol. 48, no. 1, pp. 26–33, (2009).
- [37]. M. Pirmohammadi, M. Ghassemi, Effect of magnetic field on convection heat transfer inside a tilted square enclosure, *Int. Commun. Mass* 36, pp. 776–780, (2009).
- [38]. D.C. Lo, High-resolution simulations of magnetohydrodynamic free convection in an enclosure with a transverse magnetic field using a velocity–vorticity formulation, *Int. Commun. Mass* 37, pp. 514–523, (2010).
- [39]. M. Sathiyamoorthy, A.J. Chamkha, Effect of magnetic field on natural convection flow in a liquid gallium filled square cavity for linearly heated side wall(s), *Int. J. Therm. Sci.* 49, pp. 1856–1865, (2010).
- [40]. Ridha Djebali, Mohamed El Ganaoui and Taoufik Naffouti, A 2D Lattice Boltzmann Full Analysis of MHD Convective Heat Transfer in Saturated Porous Square Enclosure, *CMES*, vol.84, no.6, pp.499-527, (2012).
- [41]. Jing, Zhao, Ni, Ming-Jiu, Wang, Zeng-Hui, Numerical study of MHD natural convection of liquid metal with wall effects. *Numer. Heat Transf. A: Appl.* 64 (8), pp. 676–693, (2013).
- [42]. Yu, P.X., Qiu, J.X., Qin, Q., Tian, Z.F., Numerical investigation of natural convection in a rectangular cavity under different directions of uniform magnetic field. *Int. J. Heat Mass Transf.* 67, pp. 1131–1144, (2013).
- [43]. Kewei Song, Wenkai Li, Yang Zhou, and Yuanru Lu, Numerical Study of Buoyancy Convection of Air under Permanent Magnetic Field and Comparison with That under Gravity Field, *Mathematical Problems in Engineering*, Article ID 494585, pp. 1-13, (2014).
- [44]. Kefayati, G.H.R., Mesoscopic simulation of magnetic field effect on natural convection of power-law fluids in a partially heated cavity. *Chem. Eng. Res. Des.* 94, pp. 337–354, (2015).
- [45]. Feng, Y., Li, H., Li, L., Zhan, F., Investigation of the effect of magnetic field on melting of solid gallium in a bottom-heated rectangular cavity using the lattice Boltzmann method. *Numer. Heat Transf. A: Appl.* 69 (11), pp. 1263–1279, (2016).
- [46]. Zhang, Jing-Kui, Li, Ben-Wen, Dong, Hua, Luo, Xiao-Hong, Lin, Huan, Analysis of magnetohydrodynamics (MHD) natural convection in 2D cavity and 3D cavity with thermal radiation effects. *Int. J. Heat Mass Transf.* 112, pp. 216–223, (2017).
- [47]. Shahidul Alam, Shirazul Hoque Mollah, Abdul Alim, Kazi Humayun Kabir, Finite Element Analysis of MHD Natural Convection in a Rectangular Cavity and Partially Heated Wall, *Engineering and Applied Sciences*. Vol. 2, No. 3, pp. 53-58, (2017).
- [48]. Ali J. Chamkha and Fatih Selimefendigil, MHD Free Convection and Entropy Generation in a Corrugated Cavity Filled with a Porous Medium Saturated with Nanofluids, *Entropy*, 20, pp 1-17, (2018).
- [49]. Haritha, C.; Shekar, Balla Chandra; Kishan, Naikoti, MHD Natural Convection Heat Transfer in a Porous Square Cavity Filled by Nanofluids with Viscous Dissipation, *Journal of Nanofluids*, Volume 7, Number 5, pp. 928-938 (11) . (2018).
- [50]. Mahapatra, T. R.; Parveen, Rujda, Entropy Generation in MHD Natural Convection Within Curved Enclosure Filled with Cu-Water Nanofluid, *Journal of Nanofluids*, Volume 8, Number 5, pp. 1051-1065 (15) . (2019).
- [51]. Sajjadi, H. & Amiri Delouei, A. & Sheikholeslami, M. & Atashafrooz, M. & Succi, S., "Simulation of three dimensional MHD natural convection using double MRT Lattice Boltzmann method," *Physica A: Statistical Mechanics and its Applications*, vol. 515(C), pp. 474-496, (2019).
- [52]. He, X. and L.S. Luo, Lattice Boltzmann Model for the incompressible Navier-Stokes equation, *Journal of statistical Physics.* (88), pp. 927-944, (1997).
- [53]. S. Jani, M. Mahmoodi, M. Amini, Magnetohydrodynamic Free Convection in a Square Cavity Heated from Below and Cooled from Other Walls, *International Journal of Mechanical, Aerospace, Industrial, Mechatronic and Manufacturing Engineering* Vol:7, No:4, pp. 750-755, (2013).

Taoufik Naffouti, et. al. " Heat transfer optimization of MHD convection in enclosure heated by symmetrical heaters separated by a triangular slab via SRT-BGK model." *International Journal of Engineering Science Invention (IJESI)*, Vol. 09(09), 2020, PP 28-50. Journal DOI- 10.35629/6734